Revue des Composites et des Matériaux Avancés-Journal of Composite and Advanced Materials
Vol. 35, No. 4, August, 2025, pp. 629-634
Journal homepage: http://iieta.org/journals/rcma

Influence of Gas Flow Rate on the Structural and Optical Properties of TiO_2 Prepared by Plasma Jet Technique

Mohammed Kh. Ibrahim[1], Bilal K. Al-Rawi[2*]

[1] Ministry of Education, Anbar Education Directorate, Al Rumadi 31001, Iraq
[2] Department of Physics, College of Education for Pure Science, University of Anbar, Al Rumadi 31001, Iraq

Corresponding Author Email: sc.bilal_alrawi@uoanbar.edu.iq

https://doi.org/10.18280/rcma.350404

Received: 25 June 2025
Revised: 28 July 2025
Accepted: 20 August 2025
Available online: 31 August 2025

Keywords:
energy gap, optical properties, plasma jet, structural properties, titanium oxide

ABSTRACT

This presents TiO_2 thin film, preparation by Plasma Jet at two levels of gas flow for 1.5 L/min and 2 L/min. The properties of the obtained TiO_2 were explored. The TiO_2 in the thin film was further evidenced by EDX analysis with high Ti to O atomic concentration ratio and no element impurity was detected below the limit. The development of the TiO_2 thin film was confirmed by characterization techniques. X-ray diffraction (XRD) patterns revealed the presence of peaks related to TiO_2 of Rutile phase at planes of 110, 101, 111, 210, and 211° respectively. The different levels of flow of the gas and the effect on the properties of the Nanoparticles as characterised by XRD, FESEM and AFM showed that with the increase in flow the particle size increases and the value of root mean square (RMS) and average roughness also increases. Also for flow levels increasing the absorbance was observed in optical properties, and energy gap value was found as 3.16 for flow level 1.5 L/min and 3.08 for 2 L/min.

1. INTRODUCTION

Its unique properties, which depend on the size, are currently considered as a powerful tool and the most successful area for theoretical research, nanoparticles. The term nanoparticles refers to particles that have a diameter less than 100 nm. Metal nanoparticles (NPs) have seen a vast range of applications in various industries such as biosensing, bio-medical science, cosmetics, food, electronics, and medicine. The nanoscale hybridization of various elements is of considerable interest to scientists and researchers due to the unique physicochemical characteristics of these hybrids, such as electrical, optical, catalytic, and thermal properties [1-3]. The unique and novel properties are the result of combination of material characteristics that paired with the effect of reduction in the size of the particle from macroscale to nanoscale, increases the surface-to-volume ratio and dramatically changes physicochemical properties [4-6]. Considerable research interest has been drawn to the multifunctional characteristics of nano-structured metal oxide materials with optical, magnetic, electric and also catalytic functions. These unique characteristics make the materials highly applicable to many exciting applications [7]. TiO_2 has attracted considerable attention in recent years as a promising n-type semiconductor, particularly for addressing environmental pollutants. Its wide use is attributed to a combination of advantageous characteristics, including its affordability, chemical stability under irradiation, non-toxicity, and strong oxidative potential. These properties make it especially effective in photocatalytic processes aimed at degrading harmful substances in air and water [8]. The different methods for the synthesis of the nanoparticles include pulsed laser deposition, sol–gel preparation, chemical coprecipitation, thermal decomposition, hydrothermal, etc. [9-11]. Among the "green" methods of nanomaterial synthesis, plasma synthesis methods have recently attracted substantial attention as novel methods of nanomaterial synthesis due to different properties, in comparison with solid, liquid, and gas-phase synthesis approaches. Traditional synthesis techniques like the sol-gel and hydrothermal methods are often hindered by prolonged reaction times and the need for intricate chemical procedures, which may lead to undesired by-products or compromise the final material's purity. In comparison, the plasma jet technique presents a more streamlined and innovative approach. It facilitates the direct synthesis of nanoparticles without depending on additional chemical agents or surfactants. By utilizing high-energy plasma in a carefully controlled setting, this method ensures the rapid generation of nanomaterials with high structural integrity and minimal surface contamination [12, 13]. Plasma jet is oriented non-thermal plasma of atmospheric pressure where the plasma afterglow (plume, projectile or stream) is stretched away from the nozzle end [14, 15]. This is a method for nano-forming by jetting plasma, in this research forming nanoparticles from titanium oxide and organizing the structural and optic properties.

2. EXPERIMENTAL WORK

Figure 1 is the non-thermal plasma working system

operated at atmospheric pressure with the scale-up of small figures indicated by the bold-line rectangle inside the figure, the glowing tip of plasma jet in the beaker where argon gas come out from its tip and interacts with deionized water and immersed metal. A Ti metal slide of 7 cm × 1 cm was immersed in 5 ml deionized water inside a glass beaker and the plasma nozzle was placed at a distance of 2 cm from the surface of the liquid in the beaker. The argon gas molecules reacted with the beaker's liquid and reacted in series with the metal surface, forming the metal's nanoparticles. Experimental preparation of nanoparticles (NPs) was carried out at an argon gas flow of 1.5 to 2 L/min and an applied voltage of 16 kV with an exposure time of 6 minutes. The plasma needle, which was perpendicular to the beaker containing deionized water, was where the metal sheet lay in place. The choice of plasma jet parameters in this study was not arbitrary but based on a series of initial optimization experiments designed to identify conditions that promote both plasma stability and consistent nanoparticle formation. Among the tested configurations, the selected flow rates and discharge settings consistently yielded a steady plasma arc with minimal oscillations, which is essential for ensuring continuous and uniform energy delivery to the metallic precursor material. In the case of titanium dioxide (TiO_2) nanoparticle synthesis, these conditions facilitated efficient breakdown of the titanium precursor under high-temperature plasma. A key factor influencing the characteristics of the resulting nanoparticles is the duration of plasma exposure. Longer exposure times tend to increase the thermal energy imparted to the system, which in turn promotes extended nucleation and subsequent particle growth through mechanisms such as surface diffusion, aggregation, and coalescence. The fundamental process of nanoparticle formation in a plasma jet environment can be understood through a three-stage mechanism. Initially, high-energy collisions within the plasma cause the vaporization or atomization of titanium species. These atoms then undergo rapid nucleation in the cooling region of the plasma plume. Following this, the newly formed nuclei collide and merge to form larger particles, a process enhanced by the high kinetic energy environment. Finally, as the particles exit the plasma zone and encounter ambient oxygen, a surface oxidation reaction occurs, transforming the metallic core into titanium dioxide (TiO_2) nanoparticles. This synthesis route, therefore, enables direct control over critical material parameters such as particle size, crystallinity, and purity by simply adjusting operating conditions making the plasma jet approach both versatile and scalable for advanced nanomaterial fabrication. Thin films have been prepared to characterize as-synthesized TiO_2 nanoparticles. Glass substrate 3 × 2 cm^2 has prepared in ultrasonic waves bath by cleaning in distilled water and alcohol for 10 min only to remove contamination. This is the drop-casting method used to deposit nanoparticle solution on the substrate. To ensure the statistical reliability of the findings, three independent TiO_2 thin film samples were prepared for each experimental condition (1.5 and 2 L/min gas flow rates). All samples underwent identical plasma jet treatment under controlled parameters. The experiments were repeated, and the results demonstrated consistent trends in structural and morphological features across samples, confirming reproducibility. This strengthens the validity of the observed correlation between gas flow rates and film characteristics.

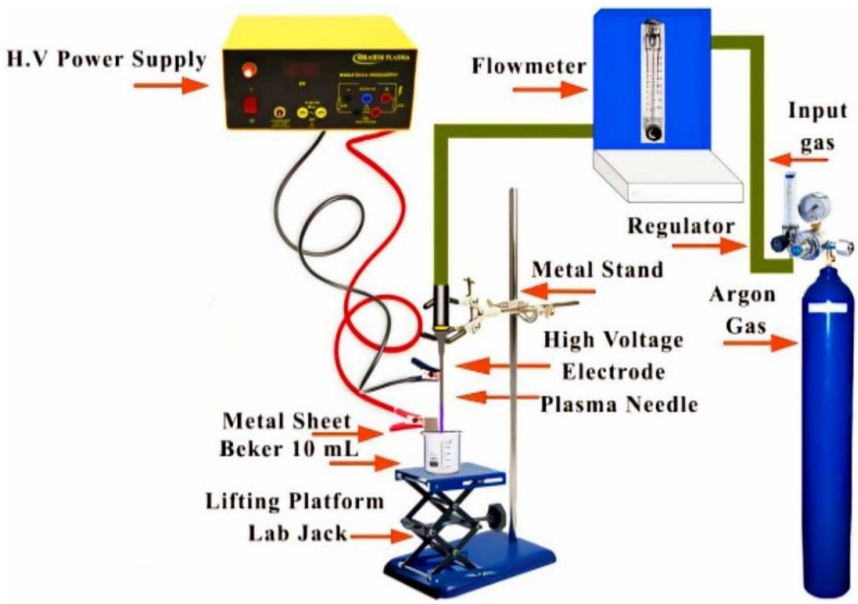

Figure 1. Experimental setup of plasma jet system

3. RESULT AND DISSECTION

It is used to find the crystal structure of the materials using X-ray. X-ray diffraction is a process where a crystalline material scatters a beam of X-rays according to its atomic arrangement, thus allowing determination of the crystal structure. Figure 2 the patterns of XRD diffraction of synthesized TiO_2 nanoparticle films on glass substrate. The diffraction pattern shown in Figure 2 proves that TiO_2 of single Rutile phase was formed were identified by matching with standard card No 96-900-4142 [16]. It is clear that the size of the crystal increases from (14.62 nm) to (15.72 nm) with the increase of gas flow rate, this is due to the fact that with the increase of gas flow rate, the crystal growth increase and that is Evident in the peaks that are clearer and more connected, in addition to the crystal purity increase. Table 1 shows the values of mean crystallite size, full width at half maximum FWHM and Miller indices (hkl).

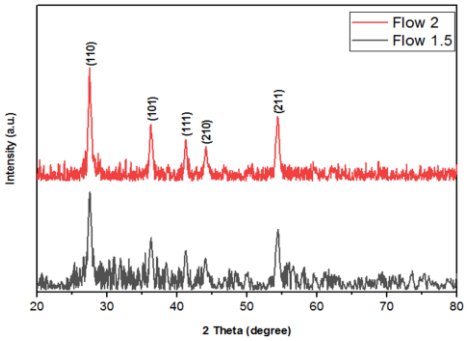

Figure 2. XRD patterns of TiO_2 with different gas flow rates

Figure 3 and Table 2 show that in TiO_2 NPs, the increased gas flow rate causes an increase in the grain size, and consequently, large crystalline grains are formed. In some cases, the value of the RMS roughness, which is a measure of surface irregularities, can also increase with the increase in the gas flow rate. Similarly, roughness average (RA) is also one of the surface roughness parameters, which might be increased due to an increase in the size of the nanoparticles as the particles will aggregate [17]. Then changes of the surface features or grain structure refinement occur, due to the increased flow. This results in higher effects and more visible changes in the texture, which makes it more efficient.

Table 1. Summary of the properties of X-rays of TiO_2 nanostructure

Gas Flow (L/Min)	2θ (Deg.)	FWHM (Deg.)	d_{hkl} Exp.(Å)	C.S (nm)	Hkl	Phase
	27.49	0.5977	3.2420	13.7	(110)	Rutile TiO_2
	36.25	0.6274	2.4761	13.3	(101)	Rutile TiO_2
1.5	41.29	0.4939	2.1848	17.2	(111)	Rutile TiO_2
	44.04	0.5862	2.0545	14.6	(210)	Rutile TiO_2
	54.39	0.6241	1.6855	14.3	(211)	Rutile TiO_2
	27.43	0.5286	3.2489	15.5	(110)	Rutile TiO_2
	36.19	0.6435	2.4801	13.0	(101)	Rutile TiO_2
2	41.18	0.4411	2.1904	19.2	(111)	Rutile TiO_2
	44.09	0.5322	2.0523	16.1	(210)	Rutile TiO_2
	54.34	0.6017	1.6869	14.8	(211)	Rutile TiO_2

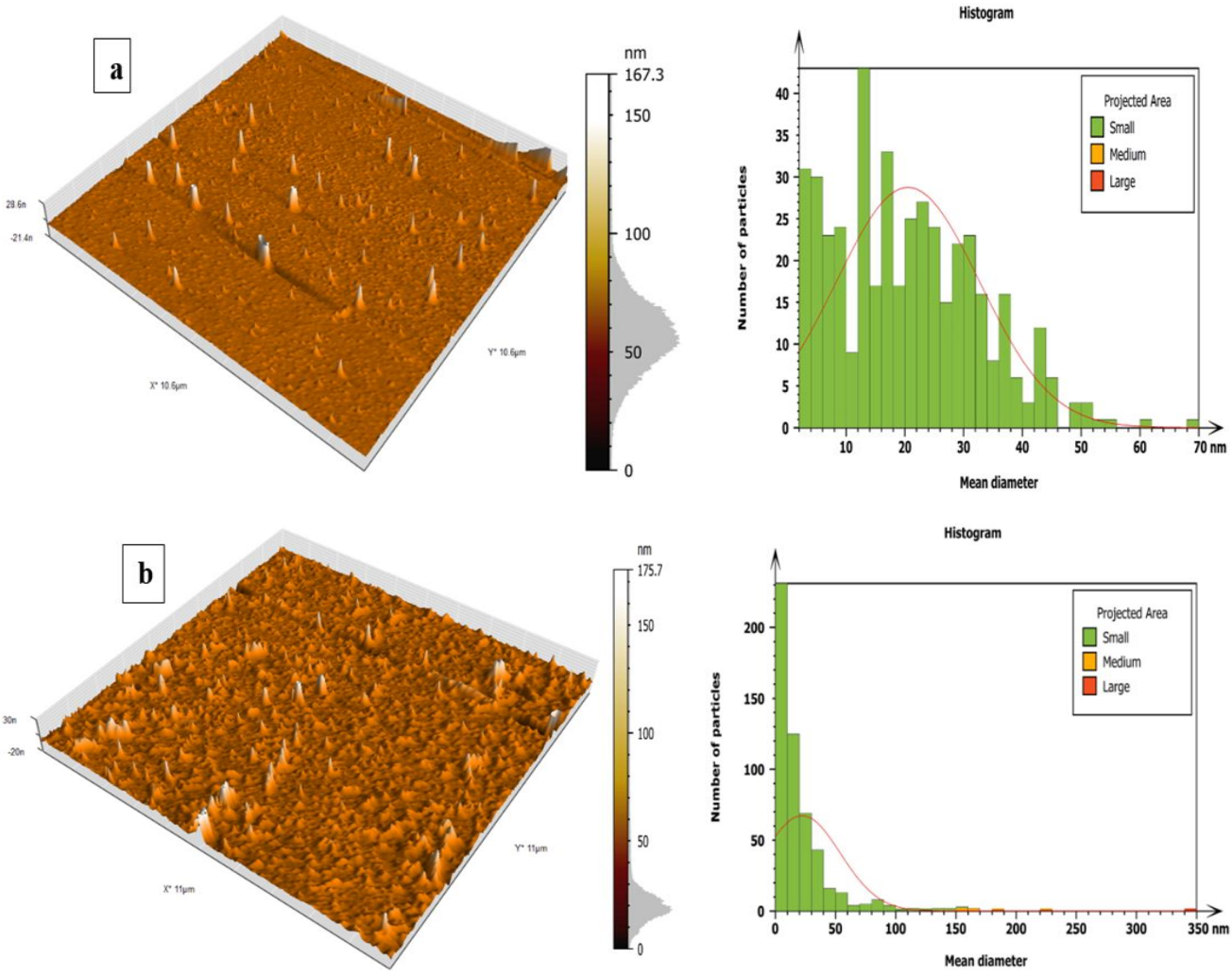

Figure 3. AFM of TiO_2 at (a) in flow 1.5 and (b) in flow 2

Table 2. Summary of AFM characteristics

Gas Flow (L/Min)	Grain Size (nm)	RMS Roughness (nm)	Roughness Ave. (nm)
1.5	20.52	5.71	3.38
2	22.22	14.82	8.35

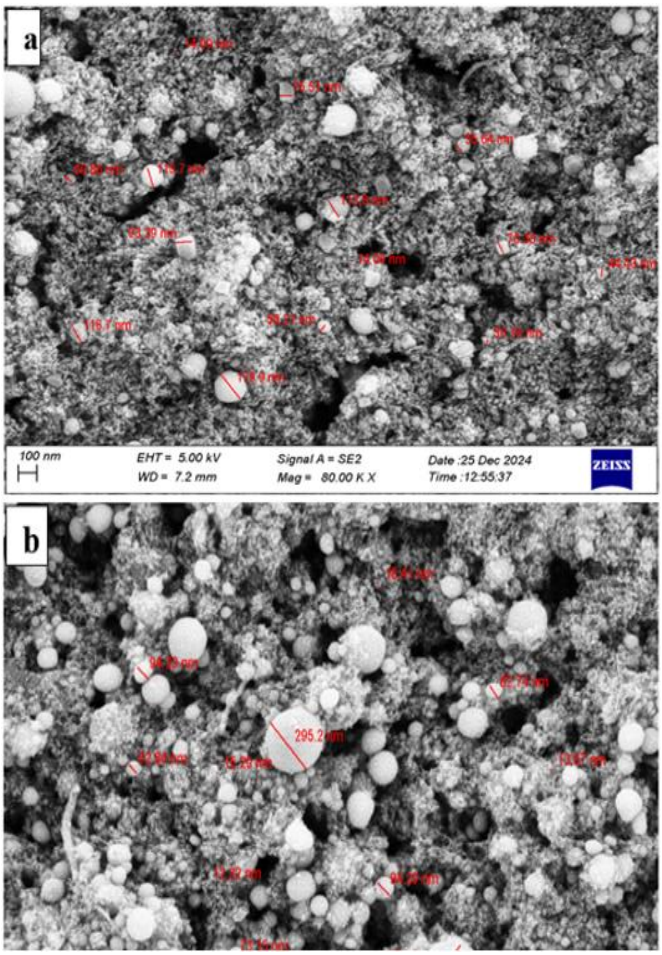

Figure 4. FESEM image of TiO_2 at (a) in flow 1.5 and (b) in flow 2

The microscopic topography of TiO_2 NPs provided in Figure 4. Field Emission Scanning Electron Microscopy (FESEM) was used to confirm the surface morphology of plasma jet prepared TiO_2 nanoparticles (NPs). The FESEM used for the magnification of the TiO_2 NPs, as shown in the image below. Through the image and zoom view, it is indicated to us that the spherical nanostructures with significant particle agglomeration confirm the homogeneity of nanoparticles in size and the Nano size of the TiO_2 NPs sample during the preparation [18]. Subsequently, when the gas flow increases, the granular size of these TiO_2 nanostructures also increases, which corresponds to the increasing average grain sizes of TiO_2 nanoparticles, where the average size of the formed nanoparticles was 74.52 nm at gas flow 1.5 and 86.87 nm at gas flow 2. The XRD and FESEM analyses provide compelling evidence that increasing the gas flow rate during the plasma-assisted synthesis of TiO_2 leads to the formation of nanoparticles with larger average diameters. This phenomenon aligns well with classical nucleation and particle growth theories. In particular, the increase in flow rate shortens the residence time of the reactive species within the high-energy plasma region. As a result, there is insufficient time for widespread nucleation to occur, leading to the formation of fewer initial nuclei. Under these conditions, the atomic and molecular species generated in the plasma tend to aggregate on a limited number of existing nuclei rather than initiating new ones. This preferential deposition leads to enhanced particle growth rather than broad nucleation, resulting in an overall increase in particle size. Moreover, it is plausible that a higher gas flow rate slightly reduces the average thermal energy within the plasma zone due to faster convective cooling. This subtle decrease in temperature may suppress the nucleation rate further while simultaneously favoring surface diffusion and accretion processes on existing particles. In such an environment, particle coalescence and grain boundary migration dominate the growth dynamics, resulting in larger and more defined nanostructures. From a material design standpoint, this insight highlights the importance of precisely tuning gas flow parameters to control particle morphology. By manipulating flow rates, researchers can engineer TiO_2 nanoparticles with specific size distributions and surface characteristics tailored for applications in photocatalysis, gas sensing, or photovoltaic systems [19, 20].

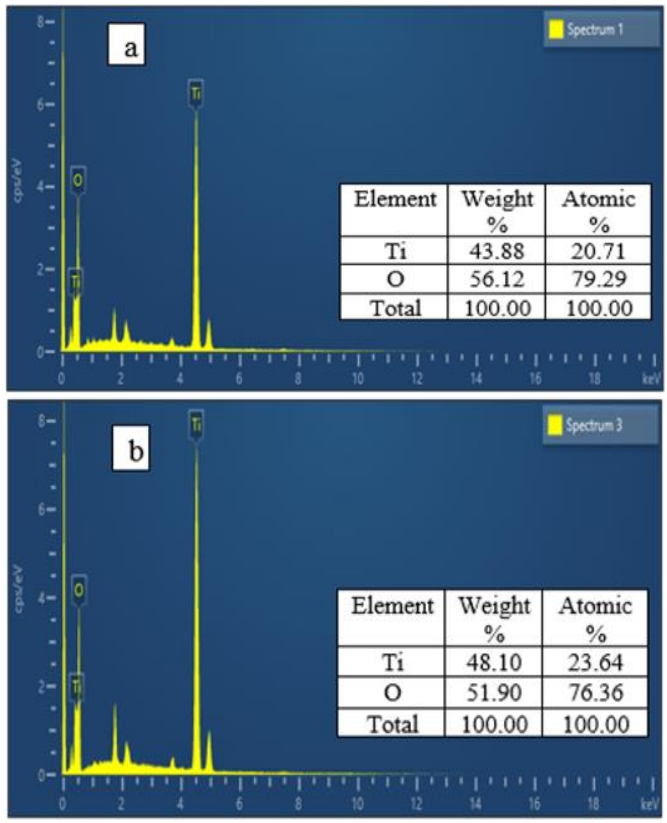

Figure 5. EDX of TiO_2 at (a) in flow 1.5 and (b) in flow 2

Energy Dispersive X-ray Spectroscopy (EDX) was used to determine the elemental composition of synthesized TiO_2 nanoparticles. Microscale EDX pattern of TiO_2 NPs [21] (Figure 5), with the details of EDX quantitative analysis depicted in an insert table as elemental weight%. At gas flow 1.5, only signals of Ti and O with mass ratios 43.88% and 56.12%, respectively, are found for TiO_2 NPs, and 48.10% and 51.90% are found at gas flow 2. The EDX did not detect any impurities of elements within its detection limit. This means that the highly pure and well crystallized fabricated TiO_2 NPs are in good agreement with the XRD data. In addition, the ratios obtained were quite close to the theoretical ones. Although the EDX spectra confirmed the presence of only Ti

and O elements, it is important to note that EDX has a limited detection threshold, especially for low atomic number elements and trace level contaminants. Therefore, the possibility of undetected impurities, such as carbon based residues or alkali metals, cannot be completely excluded. While their concentrations, if present, are likely negligible, they may still influence surface reactivity or electrical behavior. Future studies involving more sensitive techniques such as XPS.

Figure 6 shows the UV–vis absorption spectrum of the TiO_2 nanoparticle. A functional peak in the ultraviolet electromagnetic range. The presence of TiO_2 for absorbing UV (ultraviolet) light could be seen from their optical absorption less than 400 nm. A sharp absorption edge also indicates the crystalline quality of the TiO_2 NPs and confirms the narrow size distribution of the nanoparticles [22]. At the same time, TiO_2 shows increasing absorption of visible light with an increase in the flow of gas. This would support the XRD and FESEM analysis. The band gap can be determined from the following Eq. (1) as shown in Figure 7.

$$(\alpha h\nu) = A\,(h\nu - Eg)^n \qquad (1)$$

where, α is the material absorption coefficient, *h* is Planck's constant, *v* is the frequency, *Eg* is the band gap energy, and *n* is the proportionality constant and the type of sample transitions (direct or indirect) [23].

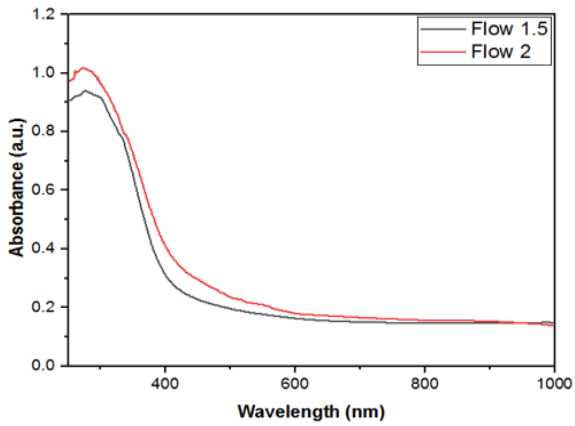

Figure 6. UV–visible absorption spectra of TiO_2

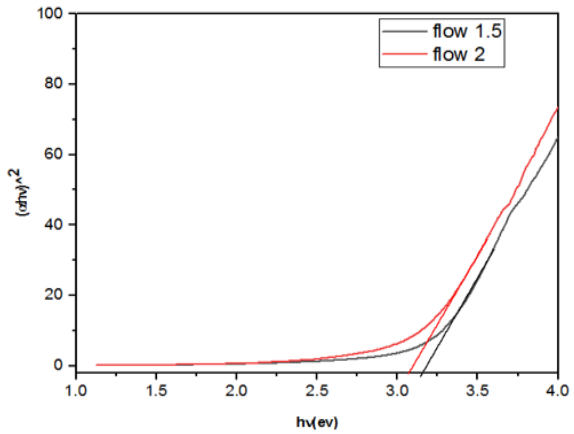

Figure 7. The measurement of the energy gap

Depending on the gas flow rate applied during the synthesis, the optical energy band gap TiO_2 Nano varies. The band gap was 3.16 at 1.5 (L/min). It dropped to 3.08 eV at 2 (L/min), further confirming the results of these prior studies [24, 25]. Increasing the granular size of the precipitant material causes an increase in height of the photonic absorption because it increases electron's energy levels by creating donor levels of energy gap and near conduction band, thus absorb large number of photons with less energy. Such variations in atomic arrangement could influence the energy band structure of the deposited material, resulting in a narrower energy gap.

4. CONCLUSIONS

The Plasma Jet technique provides an environmentally friendly, economical and readily scalable process for the production of TiO_2 thin film. By EDX analysis, this method is also in agreement with the purity of the metal oxide generated. The observed peaks for TiO_2 were of a Rutile phase as shown in XRD. Peak width at half-maximum and mean crystallite size FWHM were determined. As gas flow further increased, the crystal grain size increased and FESEM images revealed spherical nanostructures. It was discovered that the optical emitting energy gap of the Nano material changes with the gas flow used in the preparation. This research provides more than just a theoretical framework for understanding how gas flow variations influence the structure and optical behavior of TiO_2 nanoparticles during plasma jet synthesis. It opens the door to practical advancements across several high-impact applications. By precisely controlling the size and crystallinity of the nanoparticles, it becomes possible to enhance photocatalytic activity due to improved surface reactivity and tailored bandgap properties. These improvements can significantly increase the efficiency of pollutant degradation and solar energy conversion processes. Additionally, nanoparticles synthesized under optimized conditions exhibit higher stability and responsiveness in gas sensors, contributing to better detection of hazardous gases at lower concentrations. In this regard, the outcomes of the study bridge a critical gap between fundamental materials research and practical, scalable technologies.

REFERENCES

[1] Shalaan, M.M., Khalaf, M.K., Al-Rawi, B.K. (2024). Study of gold doping in optical and electrical properties of tungsten trioxide thin films deposited by spray method. Journal of Optics, 53(5): 4571-4578. https://doi.org/10.1007/s12596-024-01701-8

[2] Mustafa, A., Al-Rashid, S. (2024). Cohesive energy model for the optical properties in nanostructured materials of zinc sulfide and cadmium selenide. Chalcogenide Letters, 21(5): 407-411. https://doi.org/10.15251/CL.2024.215.407

[3] Mohammed, S.A.J., Al-Haddad, R.M., Al-Rawi, B.K. (2024). NIR laser effect on cancer cell lines activity by using Fe3O4@ Cu@ SiO2 core–shell nanoparticles. Journal of Optics, 54: 414-421. https://doi.org/10.1007/s12596-024-01676-6

[4] Mazhir, S.N., Abdalameer, N.K., Yaaqoob, L.A., Hammood, J.K. (2022). Bio-synthesis of (Zn/Se) core-shell nanoparticles by micro plasma-jet technique. International Journal of Nanoscience, 21(5): 2250041. https://doi.org/10.1142/S0219581X22500417

[5] Khathim, S.A.E., Al-Rawi, B.K., Khalaf, M.K. (2024). Surface modification of NiTi alloy with sputtered tantalum coatings to improve its hardness, corrosion resistance and biocompatibility. International Journal of Nanoscience, 23(3): 2350073. https://doi.org/10.1142/S0219581X23500734

[6] Jaffer, Z.J., Mazhir, S.N., Khalaf, M.K., Hanon, M.S. (2021). Synthesis and surface characterization of PMMA polymer films in pure oxygen, argon, and nitrogen glow discharge plasma. Journal of Physics: Conference Series, 1829: 012010. https://doi.org/10.1088/1742-6596/1829/1/012010

[7] Chouke, P.B., Shrirame, T., Potbhare, A.K., Mondal, A., et al. (2022). Bioinspired metal/metal oxide nanoparticles: A road map to potential applications. Materials Today Advances, 16: 100314. https://doi.org/10.1016/j.mtadv.2022.100314

[8] Kafel, A., Al-Rashid, S.T. (2023). Examining the impact of quantum confinement energy on the optical characteristics of zinc sulfide and gallium nitrate in the ultraviolet spectral range. Chalcogenide Letters, 20(6): 423-429. https://doi.org/10.15251/CL.2023.206.423

[9] Al-Rawi, B.K., Ramizy, A. (2019). Modeling the vibrational properties of InSb diamondoids and nanocrystals using density functional theory. Journal of Inorganic and Organometallic Polymers and Materials, 29(3): 645-650. https://doi.org/10.1007/s10904-018-1037-y

[10] Al-Rawi, B.K., Mazhir, S.N. (2023). Evaluation of antimicrobial agents of Ag–ZnO core-shell prepared by micro-jet plasma technique. International Journal of Nanoscience, 22(5): 2350044. https://doi.org/10.1142/S0219581X23500448

[11] Saleh, S.H., Alrashid, S.N.T., Khalaf, M.K. (2023). Studying the optical properties of nanostructure Au/TiO_2 bi-layer films using the SPR technique for biosensing applications. Journal of Nanostructures, 13(1): 8-15. https://doi.org/10.22052/JNS.2023.01.002

[12] Kaushik, N.K., Kaushik, N., Linh, N.N., Ghimire, B., et al. (2019). Plasma and nanomaterials: Fabrication and biomedical applications. Nanomaterials, 9(1): 98. https://doi.org/10.3390/nano9010098

[13] Alhiti, L.S., Ali, I.H. (2025). Photodetector fabrication and characterization of gold-cerium oxide nanoparticles for next-generation high-efficiency devices. Journal of Physics: Conference Series, 2974: 012033. https://doi.org/10.1088/1742-6596/2974/1/012033

[14] Hussain, A.M., Al-Rawi, B.K. (2024). Synthesis and characterizations of physical and antibacterial properties of the Ag nanoparticles by exploding of wire technique. International Journal of Nanoscience, 23(3): 2350075. https://doi.org/10.1142/S0219581X23500758

[15] Abed, H.A., Al Rashid, S.N., Mazhir, S.N. (2023). The optical and structural properties of the Fe@ Au core–shell nanoparticles prepared by PLAL. International Journal of Nanoscience, 22(6): 2330005. https://doi.org/10.1142/S0219581X23300055

[16] Thabit, W.S., Al-Rawi, B.K. (2023). The effect of atomization force on the structural properties of NiTi thin films. International Journal of Nanoscience, 22(2): 2350005. https://doi.org/10.1142/S0219581X23500059

[17] Chen, S., Jiang, Y., Zhu, Z., Zhang, Q., et al. (2024). Fluidization and application of carbon nano agglomerations. Advanced Science, 11(8): 2306355. https://doi.org/10.1002/advs.202306355

[18] Vinoth, R., Karthik, P., Devan, K., Neppolian, B., Ashokkumar, M. (2017). TiO2–NiO p–n nanocomposite with enhanced sonophotocatalytic activity under diffused sunlight. Ultrasonics Sonochemistry, 35: 655-663. https://doi.org/10.1016/j.ultsonch.2016.03.005

[19] Banerjee, S., Adhikari, E., Sapkota, P., Sebastian, A., Ptasinska, S. (2020). Atmospheric pressure plasma deposition of TiO2: A review. Materials, 13(13): 2931. https://doi.org/10.3390/ma13132931

[20] Ramkorun, B., Jain, S., Taba, A., Mahjouri-Samani, M., et al. (2024). Introducing dusty plasma particle growth of nanospherical titanium dioxide. Applied Physics Letters, 124(14): 144102. https://doi.org/10.1063/5.0186797

[21] Al-Rawi, B.K., Aljanabi, S.M. (2021). Modeling the physical properties of ZnO nanoparticles with selective hydrogen using DFT. International Journal of Nanoscience, 20(1): 2150011. https://doi.org/10.1142/S0219581X21500113

[22] Mannaa, M.A., Qasim, K.F., Alshorifi, F.T., El-Bahy, S.M., Salama, R.S. (2021). Role of NiO nanoparticles in enhancing structure properties of TiO_2 and its applications in photodegradation and hydrogen evolution. ACS Omega, 6(45): 30386-30400.

[23] Fahad, O.A., Ramizy, A., Al-Rawi, B.K. (2024). Manufacture and study CdTe/Ge/Si of broadband ultraviolet–visible photodetector. Journal of Materials Science: Materials in Electronics, 35(27): 1822. https://doi.org/10.1007/s10854-024-13544-x

[24] Cai, G., Tu, J., Zhou, D., Li, L., Zhang, J., Wang, X., Gu, C. (2014). Constructed TiO2/NiO core/shell nanorod array for efficient electrochromic application. The Journal of Physical Chemistry C, 118(13): 6690-6696. https://doi.org/10.1021/jp500699u

[25] Mohammed, S.A.J., Al-Rawi, B.K., Al-Haddad, R.M.S. (2023). Fe3O4@ SiO2 core–shell nanoparticles: Synthesis, characterization prepared by green method for Iraqi aloe vera extract. International Journal of Nanoscience, 22(2): 2350009. https://doi.org/10.1142/S0219581X23500096